A Validated Open-Source Multisolver Fourth-Generation Composite Femur Model

Alisdair R. MacLeod
Centre for Biomechanics,
Department of Mechanical Engineering,
University of Bath,
Bath BA2 7AY, UK
e-mail: a.macleod@bath.ac.uk

Hannah Rose
Centre for Biomechanics,
Department of Mechanical Engineering,
University of Bath,
Bath BA2 7AY, UK
e-mail: hannahjrose@blueyonder.co.uk

Harinderjit S. Gill[1]
Centre for Biomechanics,
Department of Mechanical Engineering,
University of Bath,
Bath BA2 7AY, UK
e-mail: r.gill@bath.ac.uk

Synthetic biomechanical test specimens are frequently used for preclinical evaluation of implant performance, often in combination with numerical modeling, such as finite-element (FE) analysis. Commercial and freely available FE packages are widely used with three FE packages in particular gaining popularity: ABAQUS (Dassault Systèmes, Johnston, RI), ANSYS (ANSYS, Inc., Canonsburg, PA), and FEBIO (University of Utah, Salt Lake City, UT). To the best of our knowledge, no study has yet made a comparison of these three commonly used solvers. Additionally, despite the femur being the most extensively studied bone in the body, no freely available validated model exists. The primary aim of the study was primarily to conduct a comparison of mesh convergence and strain prediction between the three solvers (ABAQUS, ANSYS, and FEBIO) and to provide validated open-source models of a fourth-generation composite femur for use with all the three FE packages. Second, we evaluated the geometric variability around the femoral neck region of the composite femurs. Experimental testing was conducted using fourth-generation Sawbones® composite femurs instrumented with strain gauges at four locations. A generic FE model and four specimen-specific FE models were created from CT scans. The study found that the three solvers produced excellent agreement, with strain predictions being within an average of 3.0% for all the solvers ($r^2 > 0.99$) and 1.4% for the two commercial codes. The average of the root mean squared error against the experimental results was 134.5% ($r^2 = 0.29$) for the generic model and 13.8% ($r^2 = 0.96$) for the specimen-specific models. It was found that composite femurs had variations in cortical thickness around the neck of the femur of up to 48.4%. For the first time, an experimentally validated, finite-element model of the femur is presented for use in three solvers. This model is freely available online along with all the supporting validation data.
[DOI: 10.1115/1.4034653]

Introduction

Trauma and orthopedic procedures involving the hip joint are common. In 2014, there were over 65,000 documented hip fractures and 83,000 documented hip replacement operations in England, Wales, and Northern Ireland [1,2]. This presents a huge socioeconomic burden that is projected to increase [3], and this drives the large-scale interest and use of biomechanical models of the proximal femur. These models are used for research and preclinical evaluation of treatment modalities with the aim of improving outcomes and efficacy of treatment [4,5]. Numerical models using finite-element (FE) analysis have become ubiquitous in orthopedic biomechanics. In many cases, FE analysis can provide information that would be difficult or impossible to measure experimentally [5–7]. FE analysis can also provide insight into the in vivo situation by incorporating simulation of physiological aspects or biological processes that would not be feasible in the laboratory. The evolution of image-processing software has made the generation of FE models from CT data straight-forward [7,8]. An accurate geometrical representation, however, is no guarantee of a correct model [8] and it is crucial to ensure that the model is fit for purpose. Verification of FE models, therefore, relates to the actual solving of the equations, which is influenced by modeling representation such as mesh refinement [6,9]. The model must also be validated to ensure it represents reality [10]. The gold standard is to conduct validation experiments for a direct comparison of the physical phenomena. Once the model is verified and validated, then it has the potential to be modified and generate predictive results [7].

The majority of experimental biomechanical studies relating to the proximal femur use synthetic composite test specimens (hereafter referred to as "composites") because of the advantages in terms of cost, availability, and preservation [11]. Synthetic substitutes are not able to accurately reproduce the complex structure and highly directional properties of bone. This limits their ability to predict failure loads or modes; nevertheless, Sawbones® composites are recognized as being representative of the global properties of human cortical bone in the elastic range [11–13] and will continue to be used worldwide for a range of studies. Studies using Sawbones® composites report significantly ($p < 0.02$) lower variability than cadaveric bone [11–13] with standard deviations of up to 16.3% for flexural rigidity, torsional rigidity, and axial stiffness measurements [11,12,14–16]. In comparison, the variability is between 20 and 200 times greater for cadaveric bone [13]. These studies have considered variability in terms of global measures, however, to the best of our knowledge, no data exist quantifying the variability in local properties. Variability in cortical thickness, for example, would influence strain predictions which are key to thorough validation of a model.

Despite their popularity, the only standard femur geometry freely available at present is for the third-generation Sawbones® composite [17], and there are no validated open-source models. In this context, we are using open-source to mean freely available experimental test data, geometry, and model parameters. If such a model existed for the current fourth-generation Sawbones®, it would allow researchers to use both the model and the supporting validation data, providing a valuable up-to-date preclinical tool.

While many commercial FE packages exist, two have gained popularity for biomechanical applications: ABAQUS (Dassault Systèmes, Johnston, RI) and ANSYS (ANSYS, Inc., Canonsburg, PA). There has been a move toward open-source and freely available software, such as FEBIO (University of Utah, Salt Lake City, UT), which is specifically designed for biomechanical problems, however, trust needs to be built in these open-source tools [18]. The developers of FEBIO advise that comparisons should be made against more extensively tested software for specific problems [19,20]. ABAQUS and ANSYS are two of the most well established and commonly used solvers and are thus ideal for this purpose [18]. The comparison of different solvers is important for verification, especially for problems where no analytical solution exists

[1]Corresponding author.
Manuscript received December 27, 2015; final manuscript received September 2, 2016; published online November 3, 2016. Assoc. Editor: Joel D. Stitzel.

[18]. To the best of our knowledge, no study has yet made a comparison of convergence and predictions for these three commonly used solvers related to the human femur.

The primary aim of the study was to conduct a comparison of mesh convergence and predictions between three solvers (ABAQUS, ANSYS, and FEBIO). In addition, this work set out to provide an open-source model of a composite femur that has been validated using the model format and solver specific to each FE package. We made the assumption that all the three solver codes have been verified and it is through their implementation that differences may arise. The secondary aim was to assess the composite femurs used in the study and quantify the variability in cortical thickness.

Methods

Experimental Testing. Experimental testing was conducted using fourth-generation Sawbones® composite femurs (model 3403, Biomechanical Test Materials, Pacific Research Laboratories, Malmö, Sweden). Twelve composite femurs were used in total, herein labeled F1–F12. Each composite femur was instrumented with triaxial strain gauges (SGD-2/350-RY63, Omega Engineering Limited, Manchester, UK) at four locations of interest (Fig. 1) using a custom positioning jig to ensure consistency between specimens. The composite femurs were potted using a low-melting point alloy (Wood's Metal (70 °C), Lowden Metals Ltd, Halesowen, UK) and mounted in a material testing machine (Series 5965 fitted with a 5 kN load cell; Instron, Norwood, MA). The loading vector used was that of the averaged peak hip joint reaction force during walking [21]. The resulting axes were 13.05 deg in the frontal plane and 8.16 deg in the sagittal plane (Fig. 1). The specimens were loaded up to 500 N in increments of 50 N, and the equivalent strains were calculated from the measured directional surface strains. Equivalent strain, ε_q, was defined as [22,23]

$$\varepsilon_q = \frac{1}{1+\nu}\left(\sqrt{\frac{(\varepsilon_{max}-\varepsilon_{min})^2+(\varepsilon_{min}-\varepsilon_{mid})^2+(\varepsilon_{mid}-\varepsilon_{max})^2}{2}}\right) \quad (1)$$

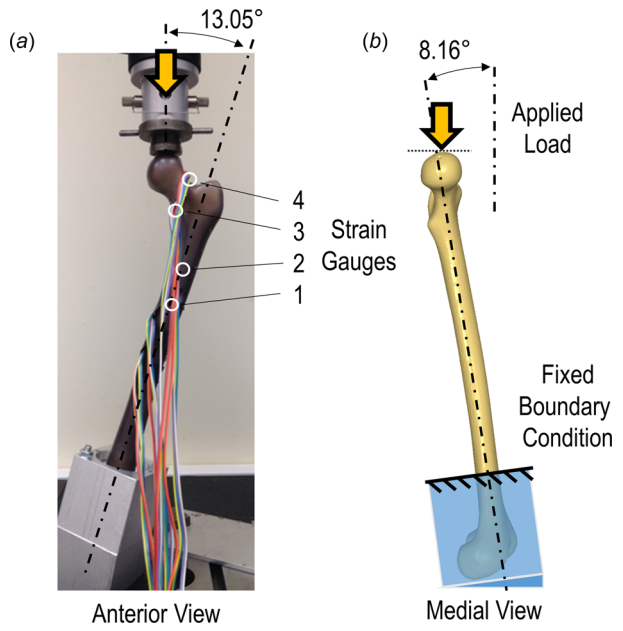

Fig. 1 (*a*) Anterior view of the experimental setup showing strain gauge locations around the femur. (*b*) Medial view of the FE model showing the loading and boundary conditions.

where ν is the Poisson's ratio of the material (see below), and ε_{max}, ε_{min}, and ε_{mid} are the maximum, minimum, and middle principle strains. The maximum and minimum principle strains were obtained from the directional surface strains using

$$\varepsilon_{max,min} = \frac{a+c}{2} \pm \frac{1}{\sqrt{2}}\left(\sqrt{(a-b)^2+(b-c)^2}\right) \quad (2)$$

where a, b, and c are the vertical, 45 deg, and horizontal directional surface strains obtained from the rosette strain gauge.

The middle principle strains were obtained by assuming plane stress conditions

$$\varepsilon_{mid} = \frac{\nu\ (a-b)}{1-\nu} \quad (2)$$

Generic FE Model. We originally intended to create and validate a single FE model using multiple Sawbones® specimens. This "generic" FE model was created based on a CT-scan (SOMATOM Sensation 64, Siemens Healthcare GmbH, Erlangen, Germany) of a fourth-generation composite femur (note that this femur was not used during experimental testing). Three-dimensional geometry (IGES format) was created using image-processing software (SCANIP version 7.0, Simpleware Ltd., Exeter, UK). The geometry was imported into ABAQUS (CAE 6.12), where the mesh, boundary conditions, and loading were specified (meshing and convergence details given later). The model was aligned to the loading vector used experimentally, and a fixed boundary condition was imposed at the location of the potting material. The model was loaded up to 500 N in 50 N increments by applying a concentrated force to the most proximal node in the vertical direction (Fig. 1). The material properties for the composite femur were taken from the manufacturer's data and the literature [14,24,25] using an average of the compressive and tensile longitudinal moduli for the cortical shell ($E = 16.35$GPa; $\nu = 0.26$) and the isotropic values for cancellous foam ($E = 137.0$MPa; $\nu = 0.3$). The experimental data collected for specimens F1–F8 were used for comparison against the predictions of the generic FE model.

Specimen-Specific FE Models. As detailed later in the "Results" section, the match between experimental data and the predictions of the generic model was not as expected. We suspected that two factors could be influencing the accuracy of the models: variability in the specimens and the alignment of the specimens in the testing machine. To address these aspects, we decided to create four specimen-specific femur models. We obtained four further composite femurs (herein referred to as F9–F12) that were instrumented with strain gauges then CT-scanned. The geometry was obtained for each femur (F9–F12), noting the location of each strain gauge from the CT scan. During the experimental testing of these four femurs, the exact locations of features such as the strain gauges and the potting material boundary were obtained using a four-camera motion capture system (Bonita B10, Vicon Motion Systems Ltd, Oxford, UK) and a pointer with five tracking spheres in accordance with the "calibrated anatomical systems technique" [26]. A custom optimization algorithm was created (MATLAB R2013b, The MathWorks Inc., Natick, MA) and used to align the FE models to the experimental condition for each femur (F9–F12). Other than the geometry and the alignment, all the aspects of the specimen-specific models were identical to the generic model described previously.

Convergence. The models were meshed using linear tetrahedral elements (ABAQUS). A mesh convergence study was performed for the generic model and one of the specimen-specific models (F10) using six mesh densities. For each level of mesh density, elements of approximately uniform size were applied throughout the model with element edge lengths: 2.8 mm, 1.2 mm, 0.9 mm, 0.75 mm, 0.6 mm, and 0.45 mm. The solution was considered to have converged if the result did not change by more than 5% for a

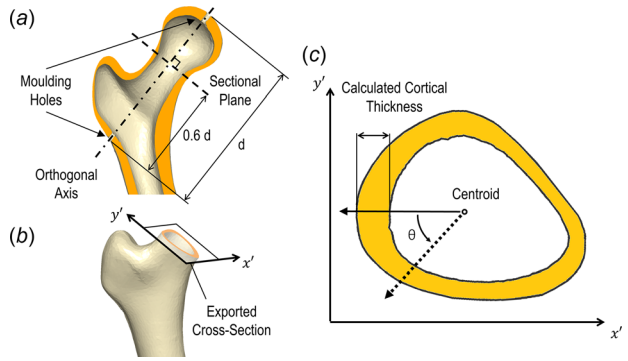

Fig. 2 (*a*) Definition of the sectional plane, (*b*) the exported cross section with nodes, and (*c*) the evaluation of the cortical thickness from the cross section

doubling of the number of elements [27]. The converged mesh resolution was 1.4×10^6 elements with average element size of 0.75 mm, and this was used for all the other specimen-specific models.

Solver Comparison. For the comparison of the three solvers, scripts were used to convert one of the femur models (F10) from an ABAQUS format into formats appropriate for the other packages. A custom python script was written to create FEBIO models (Version 2.0) from the ABAQUS models; likewise, ANSYS (Academic Research, Release 15.0) provides a script called "ABTOANS.mac," which performs this function. These scripts ensured that all the aspects of the models were identical with node-to-node equivalence. In all the cases, linear tetrahedral elements were used for ease of compatibility between solvers and to ensure a like-for-like comparison (element derivations can vary between solvers for higher order or modified elements). Implicit (quasi-static) finite analyses including nonlinear geometrical effects were conducted for all the solvers (ABAQUS/Standard; ANSYS/Mechanical Direct; and FEBIO /solid). Convergence, as described above, was performed for each of the solvers.

Cortical Thickness Evaluation. The variation in cortical thickness was evaluated at an identical cross section of the femoral neck of four femur specimens: F9–F12. The cross section was defined as the normal plane 60% of the distance between the moulding hole beneath the greater trochanter and on the femoral head (Fig. 2(*a*)). The alignment of the cross-sectional plane was scripted and determined using the moulding holes as landmarks in order to ensure consistency between specimens. SCANIP was used to generate approximately 750 nodes over the desired cross section (Fig. 2(*b*)). The periosteal and endosteal contours were acquired using the convex hull of the nodes (MATLAB) and described with approximately 150 points and 100 points for the periosteal and endosteal sections, respectively. The cross-sectional thickness was measured using the intersection of these contours with the radial line from the centroid of the cross section (Fig. 2(*c*)). This was done for eight equally spaced angular intervals (45 deg) providing eight samples of cortical thickness around the neck of composite femurs F9–F12. After testing, two material samples with cross-sectional dimensions 2 mm × 3 mm were taken from the shaft of each of these femurs ($n = 8$). Material characterization was performed using three-point bending with a span length of 45 mm (DMA 1 STAR System, Mettler Toledo, Giessen, Germany) to obtain the Young's modulus for each of the samples.

Analysis. Sensitivity studies of the FE models were conducted evaluating the influence of changes to the Young's modulus of the cortical shell, element order (linear versus quadratic), and alignment. The effect of excluding cancellous bone from the simulations was also considered.

Statistical analyses were conducted in MATLAB. The variability between strain predictions at different strain gauge locations were compared using the standard deviation (SD) of the mean. The experimentally measured strains were compared against the finite-element predictions (generic model, specimen-specific models, and solver comparison) using linear regression. The accuracy of the prediction was expressed by the coefficient of linear regression, r^2, the slope of the regression curve, and average root mean square error across all the loading increments (RMS) [5]. Bland–Altman plots were used to compare the experimental results for specimen F10 against the predictions of the three solvers using the sum of squared error (SSE), reproducibility coefficient (RPC; expressed as 1.96 times the SD), and the coefficient of variation (CV; SD of mean values).

Results

Experimental Testing and Generic FE Model. The generic FE model was not able to accurately predict the experimentally measured strains (Fig. 3(*a*)). The RMS error against the average

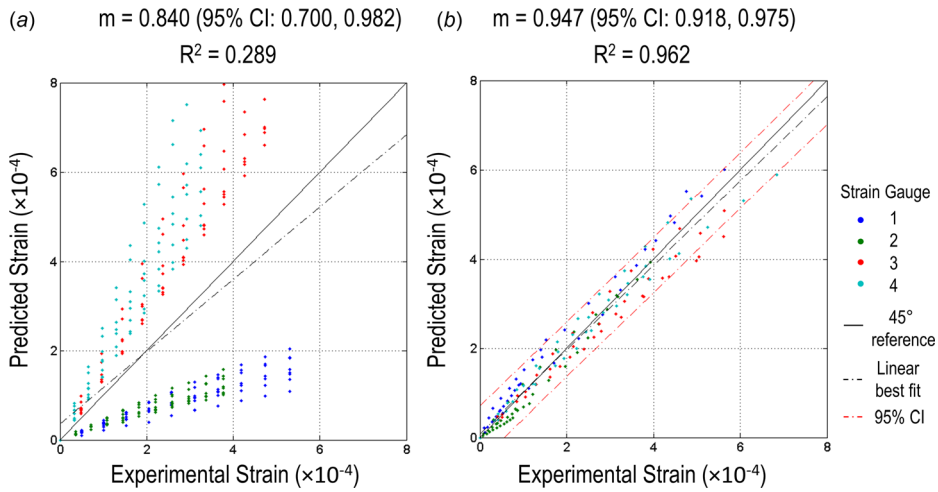

Fig. 3 (*a*) Experimental results versus generic finite-element model predictions of equivalent strain. (*b*) Experimental results versus specimen-specific finite-element predictions (specimens F9–F12) of equivalent strain. Values are shown for all the strain gauge locations at 50 N increments up to a maximum load of 500 N. N.B. least squares fit for $y = mx + c$, with values of the slope, m, given for each plot.

Table 1 Predictions of equivalent strain at the strain gauge locations around the femoral neck for specimens F9–F12

	Predicted equivalent strain around the femoral neck ($\times 10^{-3}$)					
	Specimen					
Strain gauge	F9	F10	F11	F12	Mean	STD (%)
3 (inferior)	0.562	0.460	0.499	0.564	0.521	9.72
4 (superior)	0.684	0.382	0.438	0.486	0.498	26.43

of all the experimental data was 134.5%. The slope of the linear regression was 0.840 (95% CI: 0.700, 0.982) with $r^2 = 0.289$.

Specimen-Specific FE Models. For the specimen-specific models, the RMS error of the predicted versus experimentally measured strains for all the four gauge locations was 16.8%, 5.9%, 14.1%, and 18.3% of the mean value for specimens F9–F12, respectively (average: 13.8%). The average slope of the linear regression line for all the four specimens was 0.947 (95% CI: 0.918, 0.975, $r^2 = 0.962$) (Fig. 3(*b*)). The values of slope (and correlation coefficient) for the individual composite femurs were: 0.87 ($r^2 = 0.96$); 1.06 ($r^2 = 0.99$); 0.96 ($r^2 = 0.96$); and 1.00 ($r^2 = 0.97$) for specimens F9–F12, respectively. We found that the SD in equivalent strain predictions at strain gauge locations 3 and 4 (on the femoral neck) was 9.7% and 26.4% of the mean, respectively (Table 1).

Comparison of Solvers and Convergence. For all the three solvers, the equivalent strain predictions for FE model F10 were found to converge at all the strain gauge locations using 1.4×10^6 elements or an average element size of 0.75 mm (Fig. 4). The change in predicted equivalent strain for a doubling in the number of elements was less than 2.4% for all the strain gauge locations

Table 2 Predictions of vertical displacement at the loaded node for the different solvers

	Vertical displacement at loaded node	Difference versus ABAQUS (%)
ABAQUS	−0.6330	—
ANSYS	−0.6330	0.005
FEBIO	−0.6135	−3.08

in all the solvers. The three solvers produced excellent agreement in displacement predictions at the point of load application, being within 3.1% of one another (Table 2). For the two commercial solvers, this difference was less than 0.01%. The equivalent strains at matching locations were found to be within an average of 3.0% for all the solvers ($r^2 > 0.99$). For the two commercial solvers, this difference was only 1.4% (Table 3). The predictions for all the three solvers closely matched the experimentally measured strains at all the four strain gauge locations with linear regression producing slopes of 1.038 ($r^2 = 0.984$), 1.048 ($r^2 = 0.980$), and 1.003 ($r^2 = 0.985$) for ABAQUS, ANSYS, and FEBIO, respectively (Fig. 5). The Bland–Altman plots demonstrate that the limits of agreement (±1.96 SD) matched very closely and that there was less than 3% difference in coefficient of variation (CV) and reproducibility coefficient (RPC) for all the solvers (Fig. 5).

Cortical Thickness Evaluation. The composite femurs (F9–F12) were found to have substantial variation in cortical thickness around the neck of the femur (Fig. 6). At eight locations around the femoral neck, the standard deviation in cortical thickness was between 7.0% and 16.1% of the mean value (Table 4). At each of the eight locations, the percentage difference between the thickest cross section and the thinnest was between 17.9% and 48.4%. The material characterization evaluation demonstrated that the standard deviation in Young's modulus was less than 8% of the mean for the eight samples.

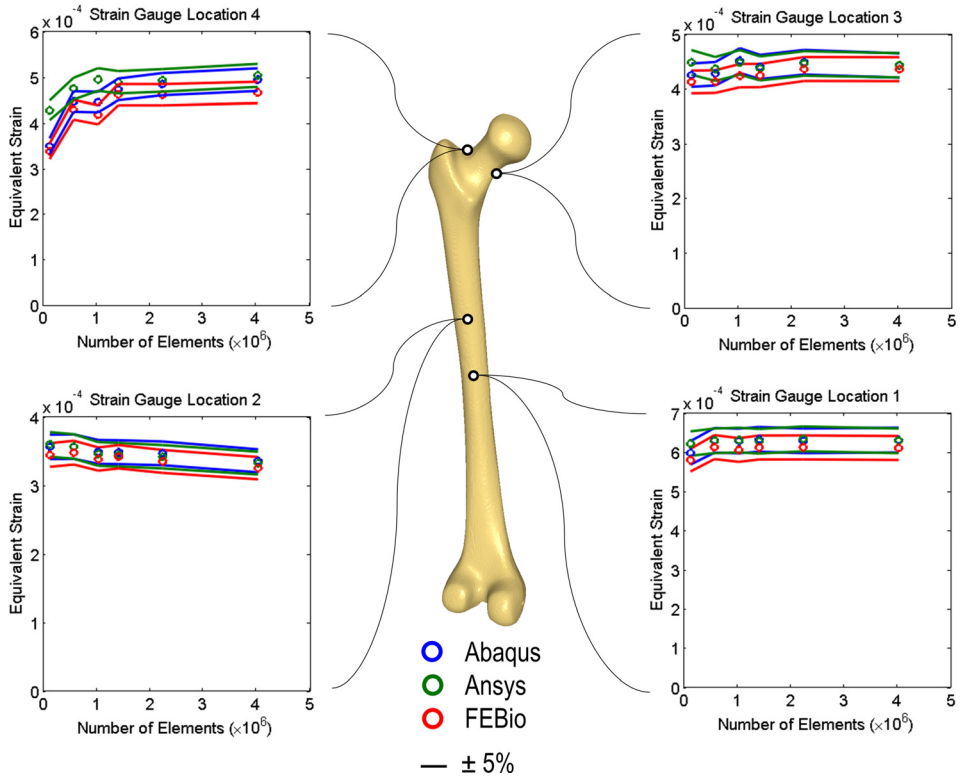

Fig. 4 Mesh convergence for the four strain gauge locations showing ±5% bounds of the equivalent strain predictions

Table 3 Equivalent strain predictions at each of the strain gauge locations for the different solvers

	Strain gauge 1	Difference versus ABAQUS (%)	Strain gauge 2	Difference versus ABAQUS (%)	Strain gauge 3	Difference versus ABAQUS (%)	Strain gauge 4	Difference versus ABAQUS (%)
ABAQUS	6.32×10^{-4}	—	3.48×10^{-4}	—	4.40×10^{-4}	—	4.73×10^{-4}	—
ANSYS	6.27×10^{-4}	−0.76	3.44×10^{-4}	−1.07	4.37×10^{-4}	−0.61	4.88×10^{-4}	3.17
FEBIO	6.11×10^{-4}	−3.40	3.41×10^{-4}	−1.96	4.24×10^{-4}	−3.69	4.61×10^{-4}	−2.51

Sensitivity. The full results of the sensitivity analyses are given in the accompanying Appendix, however, some aspects are included in the "Discussion" section.

Discussion

This study aimed to provide a validated, meshed, open-source model of the femur for use in three commonly used FE packages: ABAQUS, ANSYS, and FEBIO. As far as the authors are aware, this is the first comparison of this kind for the three FE solvers considered. During the course of the study, we attempted to create a generic composite femur model, but found that it was unable to accurately predict the experimentally measured strains. We attributed this to the lack of specimen-specific geometry and errors in alignment. By creating specimen-specific models, precisely aligned to the experimental tests (specimens F9–F12), the error against the experimentally measured strains was substantially reduced.

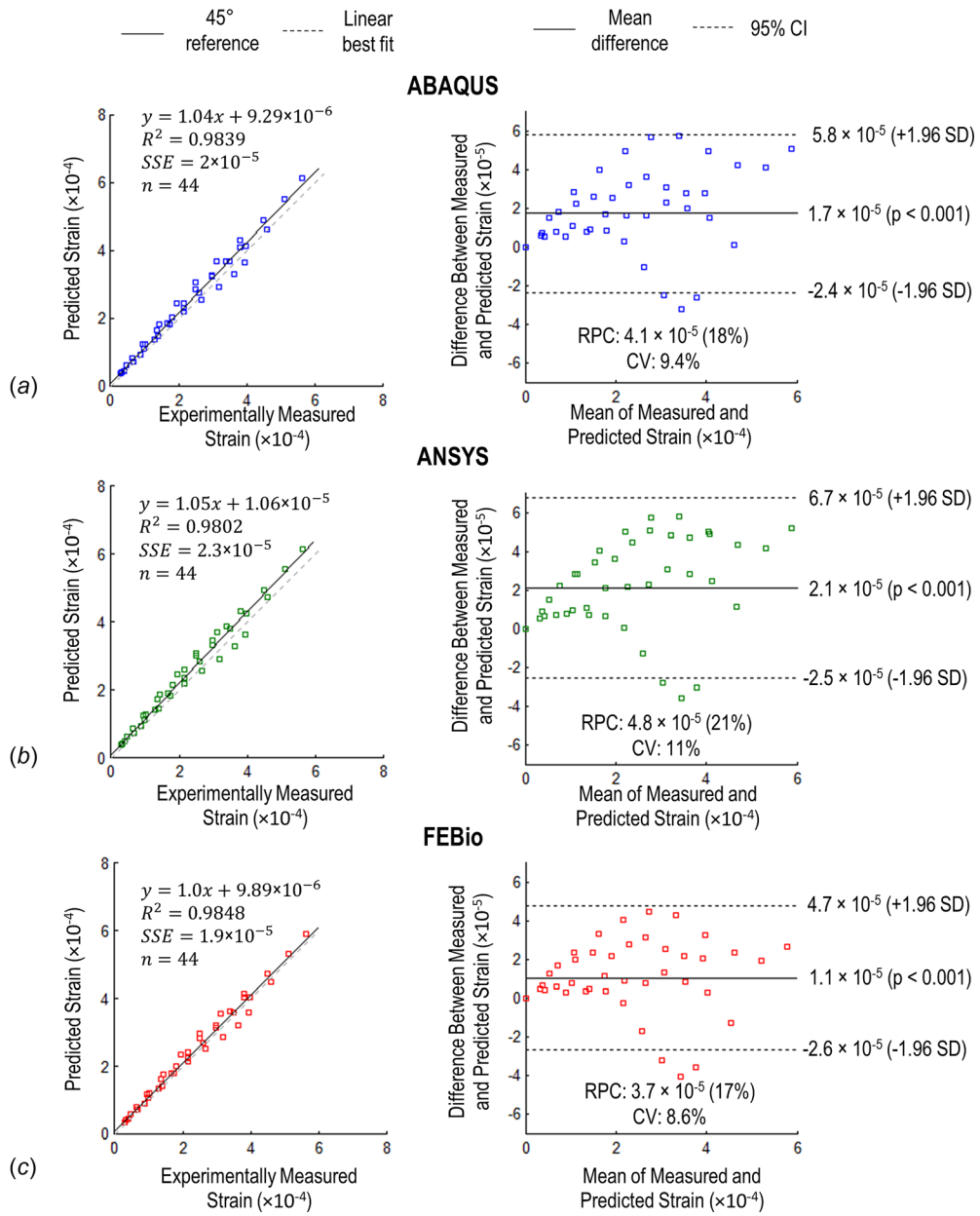

Fig. 5 Linear regression of the experimentally measured strains versus FE predictions for specimen F10 and Bland–Altman plots for the three solvers: (*a*) ABAQUS, (*b*) ANSYS, and (*c*) FEBio

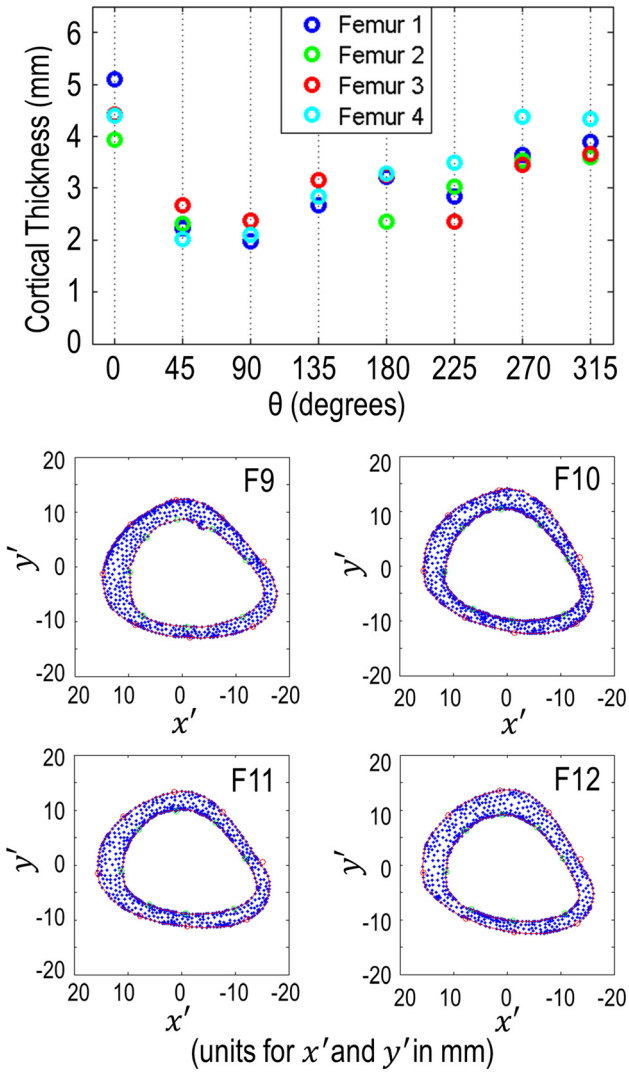

Fig. 6 Cross sections of four composite femur specimens (F9–F12), obtained as shown in Fig. 2(*b*), showing the eight locations on the inner and outer surfaces used to determine cortical thickness. Plot of cortical thickness at the eight locations around the femoral neck.

We present an FE model that has been validated against experimentally measured strains using the three solvers (specimen F10; this model is provided in formats suitable for ABAQUS, ANSYS, and FEBIO). The slope of the linear regression line (and correlation coefficient) was 1.038 ($r^2 = 0.984$), 1.048 ($r^2 = 0.980$), and 1.003 ($r^2 = 0.985$) for ABAQUS, ANSYS, and FEBIO, respectively. We will provide the supporting data and experimental results with the open-source models. We found that the three solvers produced very good agreement in terms of convergence and absolute equivalent strain predictions. FEBIO has been previously found to vary slightly against ABAQUS for specific problems [20]; we also found that FEBIO produced slightly lower strains than the two commercial packages. As expected, the two commercial software evaluated in this study were almost identical in their strain predictions.

Throughout the literature, Sawbones® composites are commonly used in biomechanical modeling due to their high degree of repeatability in mechanical testing, which allows for smaller differences to be characterized with fewer samples [13]. We chose to use Sawbones® for this reason. The use of cadaveric bone has other limitations in simulation; when using CT-based properties, the Young's moduli of each element is associated with apparent density and the material properties become mesh dependent [28]. Moreover, correctly assessing the apparent density, and therefore Young's modulus of the bone, is also important [29]. Sawbones® femurs have the advantage of being homogeneous composites, and thus, any models replicating them retain mesh-independent material properties. The material properties of Sawbones® composites have been demonstrated to be representative of the elastic behavior of human bone [11,14], and the strains within the femur have been shown to be in the elastic range during daily activities [30,31].

It should be noted that the manufacturer's data state that Sawbones® models exhibit transverse isotropy [32]; despite this, most studies use isotropic properties [33–39]. Grassi et al. attributed their modeling accuracy ($r^2 = 0.91$) to the use of orthotropic properties [40], however, we found that the inclusion of orthotropic properties only improved the strain predictions at the locations of interest by less than 5% compared to the isotropic material properties (see the Appendix). To date, no study has incorporated different properties in compression and tension described by the manufacturer [24]; we believe that this aspect could also be influential. Some studies have noted that values of Young's modulus in composite bones can be considerably lower than those described by the manufacturer [35,41], however, we used the properties given by the manufacturer and our results did not seem to be affected. Fourth-generation Sawbones® composites also are known to exhibit viscoelasticity [42]. Although our experimental tests were conducted over a relatively short time period (approximately 3 min), it is possible that inclusion of this effect could influence the predictions of our FE models.

One potential source of error in biomechanical testing is experimental alignment. In general, most human bones do not have a consistently identifiable datum; thus, consistency in load application and restraint is not straight-forward [43]. Any misalignment introduced can influence applied moments and thus stress–strain predictions [7]. We aligned the orientation of the finite-element models to the experimental setup using an optical tracking system

Table 4 Cortical thickness measurements around the femoral neck for specimens F9–F12 using the method described in Fig. 2

	Cortical thickness (mm)								
	Specimen								
Location (deg)	F9	F10	F11	F12	Range (max–min)	Maximum difference (percentage larger than min)	Mean	SD	SD (percentage of mean)
0	5.09	3.93	4.42	4.39	1.16	29.6	4.46	0.48	10.7
45	2.22	2.32	2.66	2.02	0.64	31.9	2.30	0.27	11.7
90	1.98	2.37	2.37	2.11	0.39	19.8	2.21	0.19	8.8
135	2.68	2.84	3.16	2.83	0.48	17.9	2.88	0.20	7.0
180	3.21	2.36	3.26	3.29	0.93	39.4	3.03	0.45	14.8
225	2.84	3.02	2.35	3.49	1.14	48.4	2.92	0.47	16.1
270	3.65	3.53	3.44	4.38	0.94	27.4	3.75	0.43	11.4
315	3.89	3.60	3.66	4.33	0.73	20.2	3.87	0.33	8.5

and an optimization algorithm. This also demonstrates a potential application of the open-source FE model presented in this paper, to perform sensitivity studies prior to experimental testing. It is useful to know how sensitive an experiment will be to variables such as loading angle or alignment [7]. Additionally, it is possible that the contact between the loading actuator and the femoral head provided some horizontal or rotational restraint during experimental testing; this was not included in the FE models. We conducted sensitivity studies for many aspects of the model including the influence of specimen alignment, presence of cancellous foam, the Young's modulus of cortical shell, orthotropic material properties, element type, and geometrically nonlinear analysis (see Supplement and Appendix for data).

The interpretation of all the model variables should be clear so that the model is clinically useful [9]. We chose to use equivalent strain, calculated from strain gauge readings, as it provides a scalar measure of shape distortion. Digital image correlation (DIC) has also been used to validate models across a larger field of measurement [38]. Imaging techniques do not suffer from the reinforcement effect of the strain gauges but are still not as accurate, particularly in regions of significant curvature [40]. Previous studies using DIC have validated FE models using fourth-generation composite Sawbones® femurs [38,40], with r^2 values for FE versus experimentally measured strains (equivalent and principal) ranging from 0.86 to 0.91. Previous studies using cadaveric bone with strain gauges have reported r^2 values between 0.92 and 0.96 [29,44–46]. Our results are comparable to these studies, producing r^2 values of 0.96, 0.99, 0.96, and 0.97 for specimens F9–F12, respectively. It should be noted that the spread of the predictions was reduced slightly by including orthotropic properties, with an average reduction in error of 0.9% (see the Appendix).

Evaluation of Variations in Cortical Thickness. Our sensitivity study on alignment indicated that the variability in the predictions at the proximal strain gauges was most likely due to geometric variations between the specimens. Variations in cortical thickness were assessed for specimens F9–F12, and the standard deviation in cortical thickness of the specimens was found to be up to 16.1% of the mean. The variation in strain measurements for femurs F9–F12 was similar with a standard deviation 9.7% and 26.4% of the mean for strain gauges 3 and 4, respectively. Although specimen alignment will also have a role, this indicates that cortical thickness is highly influential. Previous studies have found variability in fourth-generation Sawbones® femurs with standard deviations of up to 16.3% for flexural rigidity, torsional rigidity, and axial stiffness measurements [11,12,14]. Structural rigidity, however, is relatively insensitive to small fluctuations in local material thickness, as it is determined by properties such as the second moment of area and elastic modulus. We infer, therefore, that the variability in cortical thickness found by our study cannot account for the variations in global load–displacement response observed in these studies. On the other hand, variations in principal strain distribution, such as those found by Grassi et al. [40], will certainly be influenced by differences in cortical thickness. Therefore, depending on the research questions to be addressed by future studies, these variations should be appreciated, particularly if validation relies upon strain gauge readings made in the femoral neck region.

Conclusion

The three FE packages considered, ABAQUS, ANSYS, and FEBIO, were able to produce consistent results with regard to strain prediction and convergence. An experimentally validated finite-element model of the femur is presented for use in these three software packages. These models are freely available online at the website.[2] We have also provided the measured strain data (actual gauge readings and equivalent strains) for the F10 specimen-specific model so that future studies can reproduce the validation conducted by this study or conduct validation of their own models. Variations in cortical thickness between fourth-generation Sawbones® models exist; they play a role in producing variability in strain gauge measurements around the femoral neck. Future studies relying on such measurements need to account for this variability when using composite test specimens.

[2]http://doi.org/10.15125/BATH-00239

Acknowledgment

We gratefully acknowledge the help of Di Pressdi at the Royal United Hospital in Bath for providing the CT scans of the composite femurs used in the study.

This study was funded by the University of Bath.

Nomenclature

CV = coefficient of variation
E = Young's modulus
r^2 = coefficient of determination
RMS = root mean squared
RPC = reproducibility coefficient
SD = standard deviation
SSE = sum of squared error
ν = Poisson's ratio
ε_{max} = maximum principle strain
ε_{mid} = middle principle strain
ε_{min} = minimum principle strain
ε_q = equivalent strain

Appendix

Table 5 Influence of incorporating orthotropic properties in FE model F10. Strain values with the best match to experimental data within a one element distance (approximately 0.75 mm) of the true SG location. Values of strain shown for FE model F10 a load of 500 N.

	Equivalent strain				
Strain gauge location	Experimental measurement	Orthotropic prediction	Isotropic Prediction	Experimental vs. orthotropic (% difference)	Experimental vs. isotropic (% difference)
1	5.63E-04	5.96E-04	5.66E-04	5.77	0.51
2	3.93E-04	3.77E-04	3.38E-04	−4.17	−14.14
3	4.60E-04	4.33E-04	4.45E-04	−5.88	−3.33
4	3.82E-04	4.00E-04	4.07E-04	4.63	6.50
Mean				5.11	6.12

Table 6 Influence of ignoring cancellous bone on equivalent strain predictions. Values of strain shown for FE model F10 a load of 500 N.

	Equivalent strain prediction		
Strain gauge location	With cancellous foam	Without cancellous foam	Difference (%)
1	6.33E-04	6.33E-04	−0.02
2	3.31E-04	3.31E-04	−0.04
3	4.38E-04	4.31E-04	−1.71
4	4.75E-04	6.04E-04	27.17

Table 7 Influence of changes to Young's modulus of cortical shell on equivalent strain predictions. Values of strain shown for FE model F10 a load of 500 N.

	Young's modulus		
Strain gauge location	16350	14715	Difference (%)
1	6.33E-04	7.09E-04	12.00
2	3.31E-04	3.72E-04	12.26
3	4.38E-04	4.87E-04	11.00
4	4.75E-04	5.18E-04	9.12
	Mean (%)		11.09

Table 8 Influence of element type on equivalent strain predictions. Values of strain shown for FE model F10 a load of 500 N.

	Equivalent strain prediction		
Strain gauge location	Linear elements	Quadratic element	Difference (%)
1	6.33E-04	5.99E-04	−5.40
2	3.31E-04	3.21E-04	−2.94
3	4.38E-04	4.47E-04	2.01
4	4.75E-04	4.69E-04	−1.25
	Mean (%)		2.90

Table 9 The influence of changes in alignment in the frontal and sagittal planes on equivalent strain predictions. Values of strain shown for FE model F10 a load of 500 N.

		One degree rotation in:		Change in strain prediction (%)	
Strain gauge location	Model F10 prediction	Frontal plane	Sagittal plane	Frontal	Stagittal
1	6.33E-04	7.81E-04	7.69E-04	23.4	21.6
2	3.31E-04	4.14E-04	4.15E-04	25.0	25.5
3	4.38E-04	4.88E-04	5.07E-04	11.2	15.6
4	4.75E-04	5.14E-04	5.49E-04	8.2	15.6

Table 10 Influence of nonlinear geometrical effects on equivalent strain predictions. Values of strain shown for FE model F10 a load of 500 N.

	Equivalent strain prediction		
Strain gauge location	Including nonlinear geometrical effects	Excluding nonlinear geometrical effects	Difference (%)
1	6.33E-04	5.91E-04	−7.08
2	3.31E-04	3.02E-04	−9.53
3	4.38E-04	4.45E-04	1.43
4	4.75E-04	4.77E-04	0.44
	Mean (%)		−3.69

References

[1] Royal College of Physicians, 2015, "National Hip Fracture Database (NHFD) Annual Report," Royal College of Physicians, London.

[2] NJR Steering Committee, 2015, "National Joint Registry for England, Wales, Northern Ireland: 12th Annual Report," NJR Steering Committee, Hemel Hempstead, UK.

[3] Fernandez, M. A., Griffin, X. L., and Costa, M. L., 2015, "Hip Fracture Surgery," Bone Joint J., **97-B**(7), pp. 875–879.

[4] Miles, B., Kolos, E., Walter, W. L., Appleyard, R., Li, Q., Chen, Y., and Ruys, A. J., 2015, "Subject-Specific Finite Element Model With an Optical Tracking System in Total Hip Replacement Surgery," Proc. Inst. Mech. Eng., Part H, **229**(4), pp. 280–290.

[5] Taddei, F., Cristofolini, L., Martelli, S., Gill, H. S., and Viceconti, M., 2006, "Subject-Specific Finite Element Models of Long Bones: An In Vitro Evaluation of the Overall Accuracy," J. Biomech., **39**(13), pp. 2457–2467.

[6] Anderson, A. E., Ellis, B. J., and Weiss, J. A., 2007, "Verification, Validation and Sensitivity Studies in Computational Biomechanics," Comput. Methods Biomech. Biomed. Eng., **10**(3), pp. 171–184.

[7] Cristofolini, L., Schileo, E., Juszczyk, M., Taddei, F., Martelli, S., and Viceconti, M., 2010, "Mechanical Testing of Bones: The Positive Synergy of Finite-Element Models and In Vitro Experiments," Philos. Trans. Ser. A, **368**(1920), pp. 2725–2763.

[8] Prendergast, P. J., 1997, "Finite Element Models in Tissue Mechanics and Orthopaedic Implant Design," Clin. Biomech., **12**(6), pp. 343–366.

[9] Viceconti, M., Olsen, S., Nolte, L. P., and Burton, K., 2005, "Extracting Clinically Relevant Data From Finite Element Simulations," Clin. Biomech., **20**(5), pp. 451–454.

[10] Babuska, I., and Oden, J. T., 2004, "Verification and Validation in Computational Engineering and Science: Basic Concepts," Comput. Methods Appl. Mech. Eng., **193**(36–38), pp. 4057–4066.

[11] Elfar, J., and Stanbury, S., 2014, "Composite Bone Models in Orthopaedic Surgery Research and Education," J. Am. Acad. Orthop. Surg., **22**(2), pp. 111–120.

[12] Gardner, M. P., Chong, A. C. M., Pollock, A. G., and Wooley, P. H., 2010, "Mechanical Evaluation of Large-Size Fourth-Generation Composite Femur and Tibia Models," Ann. Biomed. Eng., **38**(3), pp. 613–620.

[13] Cristofolini, L., Viceconti, M., Cappello, A., and Toni, A., 1996, "Mechanical Validation of Whole Bone Composite Femur Models," J. Biomech., **29**(4), pp. 525–535.

[14] Heiner, A. D., 2008, "Structural Properties of Fourth-Generation Composite Femurs and Tibias," J. Biomech., **41**(15), pp. 3282–3284.

[15] Dunlap, J. T., Chong, A. C. M., Lucas, G. L., and Cooke, F. W., 2008, "Structural Properties of a Novel Design of Composite Analogue Humeri Models," Ann. Biomed. Eng., **36**(11), pp. 1922–1926.

[16] Grover, P., Albert, C., Wang, M., and Harris, G. F., 2011, "Mechanical Characterization of Fourth Generation Composite Humerus," Proc. Inst. Mech. Eng., Part H, **225**(12), pp. 1169–1176.

[17] Viceconti, M., Casali, M., Massari, B., Cristofolini, L., Bassini, S., and Toni, A., 1996, "The 'Standardized Femur Program' Proposal for a Reference Geometry to be Used for the Creation of Finite Element Models of the Femur," J. Biomech., **29**(9), p. 1241.

[18] Meng, Q., Jin, Z., Fisher, J., and Wilcox, R., 2013, "Comparison Between FEBio and Abaqus for Biphasic Contact Problems," Proc. Inst. Mech. Eng., Part H, **227**(9), pp. 1009–1019.

[19] Maas, S. A., Ellis, B. J., Rawlins, D. S., and Weiss, J. A., 2009, "A Comparison of FEBio, ABAQUS, and NIKE3D Results for a Suite of Verification Problems," SCI Institute Technical Report No. UUSCI-2009-009.

[20] Maas, S. A., Ellis, B. J., Ateshian, G. A., and Weiss, J. A., 2012, "FEBio: Finite Elements for Biomechanics," ASME J. Biomech. Eng., **134**(1), p. 011005.

[21] Bergmann, G., Deuretzbacher, G., Heller, M., Graichen, F., Rohlmann, A., Strauss, J., and Duda, G. N., 2001, "Hip Contact Forces and Gait Patterns From Routine Activities," J. Biomech., **34**(7), pp. 859–871.

[22] ANSYS, 2013, "ANSYS 15.0 Mechanical User's Guide," ANSYS, Inc., Canonsburg, PA.

[23] Agilent Technologies, 1999, "Application Note 290-1: Practical Strain Gage Measurements," Agilent Technologies, Manchester, UK, accessed May 3, 2016, www.omega.co.uk/techref/pdf/StrainGage_Measurement.pdf

[24] MatWeb, 2015, "MatWeb Material Property Data. Sawbones Technical Data Sheets," MatWeb LLC, Blacksburg, VA, accessed May 12, 2015, www.matweb.com

[25] Pacific Research Labora tories, 2015, "Sawbones Biomechanical Test Materials," Pacific Research Laboratories, Vashon, Island, WA, accessed Feb. 2, 2016, http://www.sawbones.com/UserFiles/Docs/biomechanical_catalog.pdf

[26] Cappozzo, A., Catani, F., Della Croce, U., and Leardini, A., 1995, "Position and Orientation in Space of Bones During Movement: Anatomical Frame Definition and Determination," Clin. Biomech., **10**(4), pp. 171–178.

[27] Pegg, E. C., Murray, D. W., Pandit, H. G., O'Connor, J. J., and Gill, H. S., 2013, "Fracture of Mobile Unicompartmental Knee Bearings: A Parametric Finite Element Study," Proc. Inst. Mech. Eng., Part H, **227**(11), pp. 1213–1223.

[28] Taddei, F., Schileo, E., Helgason, B., Cristofolini, L., and Viceconti, M., 2007, "The Material Mapping Strategy Influences the Accuracy of CT-Based Finite Element Models of Bones: An Evaluation Against Experimental Measurements," Med. Eng. Phys., **29**(9), pp. 973–979.

[29] Schileo, E., Dall'Ara, E., Taddei, F., Malandrino, A., Schotkamp, T., Baleani, M., and Viceconti, M., 2008, "An Accurate Estimation of Bone Density Improves the Accuracy of Subject-Specific Finite Element Models," J. Biomech., **41**(11), pp. 2483–2491.

[30] Bayraktar, H. H., Morgan, E. F., Niebur, G. L., Morris, G. E., Wong, E. K., and Keaveny, T. M., 2004, "Comparison of the Elastic and Yield Properties of Human Femoral Trabecular and Cortical Bone Tissue," J. Biomech., **37**(1), pp. 27–35.

[31] Martelli, S., Pivonka, P., and Ebeling, P. R., 2014, "Femoral Shaft Strains During Daily Activities: Implications for Atypical Femoral Fractures," Clin. Biomech., **29**(8), pp. 869–876.

[32] Pacific Research Laboratories, 2013, "Sawbones Catalog," Pacific Research Laboratories, Inc., Vashon Island, WA.

[33] Salas, C., Mercer, D., DeCoster, T. A., and Taha, M. M. R., 2011, "Experimental and Probabilistic Analysis of Distal Femoral Periprosthetic Fracture: A Comparison of Locking Plate and Intramedullary Nail Fixation—Part

B: Probabilistic Investigation," Comput. Methods Biomech. Biomed. Eng., **14**(2), pp. 175–182.
[34] Wieding, J., Souffrant, R., Fritsche, A., Mittelmeier, W., and Bader, R., 2012, "Finite Element Analysis of Osteosynthesis Screw Fixation in the Bone Stock: An Appropriate Method for Automatic Screw Modelling," PLoS One, **7**(3), p. e33776.
[35] Reimeringer, M., Nuño, N., Desmarais-Trépanier, C., Lavigne, M., and Vendittoli, P. A., 2012, "The Influence of Uncemented Femoral Stem Length and Design on Its Primary Stability: A Finite Element Analysis," Comput. Methods Biomech. Biomed. Eng., **16**(11), pp. 1221–1231.
[36] Pal, B., Gupta, S., New, A. M. R., and Browne, M., 2010, "Strain and Micromotion in Intact and Resurfaced Composite Femurs: Experimental and Numerical Investigations," J. Biomech., **43**(10), pp. 1923–1930.
[37] Pettersen, S. H., Wik, T. S., and Skallerud, B., 2009, "Subject Specific Finite Element Analysis of Stress Shielding Around a Cementless Femoral Stem," Clin. Biomech., **24**(2), pp. 196–202.
[38] Dickinson, A. S., Taylor, A. C., Ozturk, H., and Browne, M., 2011, "Experimental Validation of a Finite Element Model of the Proximal Femur Using Digital Image Correlation and a Composite Bone Model," ASME J. Biomech. Eng., **133**(1), p. 014504.
[39] Samiezadeh, S., Tavakkoli Avval, P., Fawaz, Z., and Bougherara, H., 2014, "Biomechanical Assessment of Composite Versus Metallic Intramedullary Nailing System in Femoral Shaft Fractures: A Finite Element Study," Clin. Biomech., **29**(7), pp. 803–810.
[40] Grassi, L., Väänänen, S. P., Amin Yavari, S., Weinans, H., Jurvelin, J. S., Zadpoor, A. A., and Isaksson, H., 2013, "Experimental Validation of Finite Element Model for Proximal Composite Femur Using Optical Measurements," J. Mech. Behav. Biomed. Mater., **21**, pp. 86–94.
[41] Gilroy, D., Young, A. M., Phillips, A., Wheel, M., and Riches, P. E., 2014, "Characterisation and Validation of SawbonesTM Artificial Composite Femur Material," 7th World Congress of Biomechanics, Boston, MA, ID No. 51226.
[42] Chong, A. C. M., Friis, E. A., Ballard, G. P., Czuwala, P. J., and Cooke, F. W., 2007, "Fatigue Performance of Composite Analogue Femur Constructs Under High Activity Loading," Ann. Biomed. Eng., **35**(7), pp. 1196–1205.
[43] Wu, G., Siegler, S., Allard, P., Kirtley, C., Leardini, A., Rosenbaum, D., Whittle, M., D'Lima, D. D., Cristofolini, L., Witte, H., Schmid, O., and Stokes, I., 2002, "ISB Recommendation on Definitions of Joint Coordinate System of Various Joints for the Reporting of Human Joint Motion—Part I: Ankle, Hip, and Spine," J. Biomech., **35**(4), pp. 543–548.
[44] Bessho, M., Ohnishi, I., Matsuyama, J., Matsumoto, T., Imai, K., and Nakamura, K., 2007, "Prediction of Strength and Strain of the Proximal Femur by a CT-Based Finite Element Method," J. Biomech., **40**(8), pp. 1745–1753.
[45] Trabelsi, N., Yosibash, Z., Wutte, C., Augat, P., and Eberle, S., 2011, "Patient-Specific Finite Element Analysis of the Human Femur-A Double-Blinded Biomechanical Validation," J. Biomech., **44**(9), pp. 1666–1672.
[46] Trabelsi, N., and Yosibash, Z., 2011, "Patient-Specific Finite-Element Analyses of the Proximal Femur With Orthotropic Material Properties Validated by Experiments," ASME J. Biomech. Eng., **133**(6), p. 061001.